arXiv:1608.05603v1 [cond-mat.soft] 19 Aug 2016

Cross-stream transport of asymmetric particles driven by oscillating shear

Matthias Laumann,[1] Paul Bauknecht,[2] Stephan Gekle,[2] Diego Kienle,[1,*] and Walter Zimmermann[1]

[1] *Theoretische Physik I, Universität Bayreuth, 95440 Bayreuth, Germany*
[2] *Biofluid Simulation and Modeling, Universität Bayreuth, 95440 Bayreuth, Germany*

(Dated: August 22, 2016)

We study the dynamics of asymmetric, deformable particles in oscillatory, linear shear flow. By simulating the motion of a dumbbell, a ring polymer, and a capsule we show that cross-stream migration occurs for asymmetric elastic particles even in linear shear flow if the shear rate varies in time. The migration is generic as it does not depend on the particle dimension. Importantly, the migration velocity and migration direction are robust to variations of the initial particle orientation, making our proposed scheme suitable for sorting particles with asymmetric material properties.

PACS numbers: 47.15.G-,47.57.ef,47.60.Dx,83.50.-v

Introduction. During the recent years, microfluidics has evolved to a cross-disciplinary field, ranging from basic physics to a plethora of biological and technical applications [1–7], including the control of small amounts of fluids, chemical synthesis [8, 9], biological analysis [10, 11], and the study of the deformation dynamics of droplets, vesicles, capsules, or blood cells [12–38]. An important transport mechanism in microfluidic flows is the cross-stream migration (CSM), where particles move across streamlines and can be sorted due to their particle-specific properties [39, 40].

The CSM effect has been first reported in 1961 by Segre and Silberberg for rigid particles at finite Reynolds number in pipes with diameters of several millimeters [41]. When channels approach the micrometer scale, the Reynolds number vanishes (Stokes regime) and fluid inertia does not matter; likewise, for μm-sized particles thermal effects can be discarded. In the Stokes regime, CSM arises in curvilinear [12–15] and rectilinear flow [16–20], if the particle is elastic and, in case of rectilinear flow, the flow's fore-aft symmetry is broken, requiring intra-particle hydrodynamic interaction [16–19]. Such symmetry breaking occurs near boundaries via wall-induced lift forces [19, 21–23] or by space-dependent shear rates, so that dumbbells [16–18], droplets [24–26], vesicles and capsules [27–29] exhibit CSM even in unbounded flow. These parity breaking mechanisms may be accompanied by other effects due to viscosity contrast [24, 42] or particle chirality [43], which further impact the CSM.

Here we show that a controlled cross-stream migration is possible even in unbounded *linear* shear flow, provided that (1) the particle holds an intrinsic asymmetry (parity breaking), and (2) the shear rate varies in time, causing time-dependent particle deformations. Importantly, the cross-stream migration occurs irrespective of the dimensionality of the particle, accentuating its *generic* nature, as we show by studying particles extending in one (1D), two (2D), and three (3D) dimensions. We demonstrate that the CSM depends on external flow parameters such as switching period, which can be controlled conveniently to achieve an optimized migration.

Approach. To reveal the generic behavior of the CSM in oscillatory shear flow, we use three kinds of particles, which share the common features that they are deformable, asymmetric, and their constituent parts interact hydrodynamically. The first two particle types are a dumbbell (1D) and a ring-polymer (2D), modeled by a sequence of bead-spring units and connected by linear springs with a bond length b and force constant k. The dumbbell asymmetry is modeled by assigning different friction coefficients ζ_1 and ζ_2 to unequal sized beads 1 and 2 with $r_\zeta = \zeta_2/\zeta_1 = 3$ [Fig. 1 (a): inset]. The asymmetry of the N-bead ring-polymer is realized by a space-dependent bending stiffness $\kappa(\{\mathbf{r}\})$ along the ring contour $\{\mathbf{r}\}$. The third particle is an elastic capsule (3D), the asymmetry of which is implemented likewise by a spatially varying bending stiffness $\kappa(\{\mathbf{r}\})$ along the capsule surface $\{\mathbf{r}\}$. For the purpose of this study, we split the contour/surface of the ring/capsule in equal parts (Janus-particle); the stiff and bendy portion in either case has a bending stiffness of κ_2 and κ_1 with a ratio $r_\kappa = \kappa_2/\kappa_1 = 1.5$ [Fig. 1 (b) and (c): inset].

The migration dynamics of all three particle kinds is obtained from their non-Brownian trajectories. The trajectories for the dumbbell and ring-polymer are determined by solving the Stokesian dynamics for each bead, including the hydrodynamic backflow (HB) due to the fluid-particle interaction (HI) described by the Oseen tensor [44]. The capsule path is calculated using the Immersed Boundary Method in conjunction with the Lattice Boltzmann method for the flow [45], employing an adapted version of the ESPResSo package [46]. Throughout we assume a time-dependent (td), linear shear flow $\mathbf{u}(x, y) = S(t)\, y \mathbf{e}_x$ along the $\mathbf{e}_x$-axis; the shear rate $S(t)$ has a period T with $S(t) = +\dot{\gamma}$ during the first half-period T_1 and $S(t) = -\dot{\gamma}$ during the second half-period T_2 with $T_1 = T_2 = T/2$. The initial orientation of all three particles is $\phi_0 = 2.0\pi$ with the small ζ_1-bead, respectively, the stiff κ_2-contour/surface being located to the left. The Supporting Information [47] provides further details.

Generic Behavior. Figure 1 shows the center-of-mass

position $y_c(t)$, scaled with respect to the dumbbell/ring bond length b or the capsule radius a, as a function of the scaled time $t\dot{\gamma}$ with fixed $\dot{\gamma}$ for all three particles. For symmetric particles ($r_{\zeta,\kappa} = 1.0$), the cross-stream migration is zero at any time (dashed line) [14, 17] as parity breaking does not occur irrespective of whether the shear flow is at steady-state (ss) or time-dependent (td). For

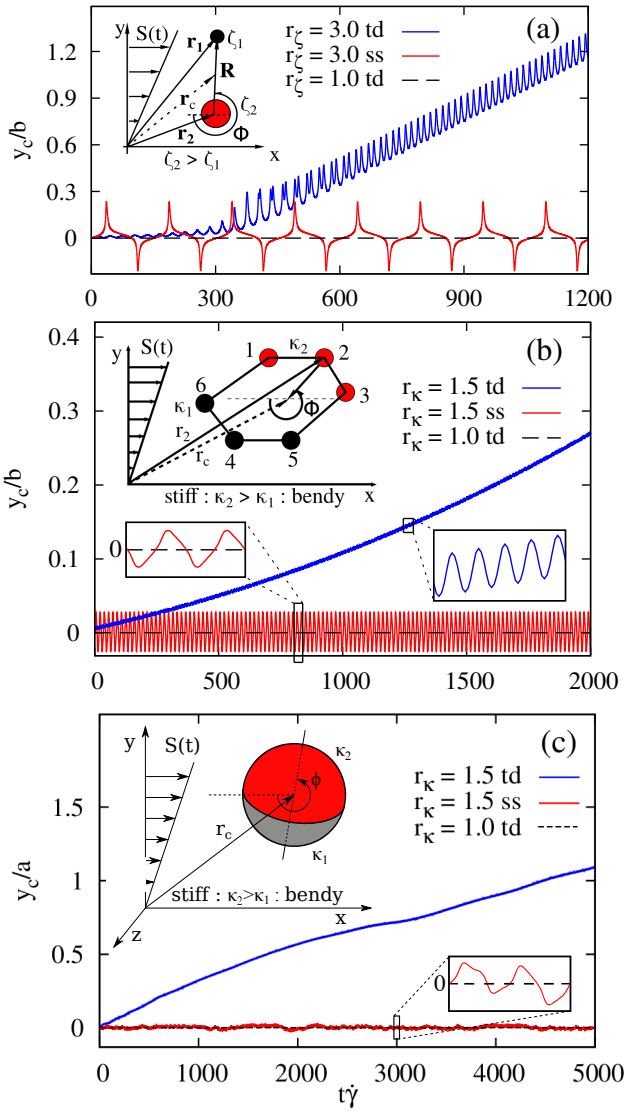

FIG. 1. (Color online) Lateral position $y_c(t)$ vs. scaled time $t\dot{\gamma}$ for the asymmetric (a) 1D dumbbell, (b) 2D ring, and (c) 3D capsule, sketches of which are shown in the inset. Irrespective of the model details, all particle types perform a *net* cross-stream migration in linear shear (blue solid), if the shear rate is time-dependent (td). At steady shear (ss), $y_c(t)$ oscillates around a constant mean (red solid), so that the net migration vanishes [14, 17]. For symmetric particles ($r_{\zeta,\kappa} = 1.0$), the migration is zero. The initial orientation is $\phi_0 = 2.0\pi$.

asymmetric particles ($r_{\zeta,\kappa} > 1.0$) in steady shear flow parity breaking exists, but which results only in an alternating CSM as reflected in the oscillatory behavior of $y_c(t)$; the *net* migration over one shear cycle, however, is still zero (red solid line). This intermittent migration of asymmetric particles can be exploited to attain a *net* cross-stream migration, if the shear rate $S(t)$ is made time-dependent by switching $S(t)$ at a frequency $1/T$, as shown in Fig. 1 (a)-(c) by the blue solid line. The fact that all three particles display cross-stream behavior irrespective of their dimensionality and model details is an indication of a *generic* property [47], which can be attributed to the different *mean* shapes the particle acquires during each half-period, as discussed next.

Migration Mechanism. To understand the CSM mechanism we use the N-bead ring as representative particle and consider the case, where the ring has approached the steady-state, i.e., for an initial orientation ϕ_0 the ring adopts (after a transient) one stable *mean* orientation $\langle\phi\rangle_T$ over one shear-cyle T. Specifically, for $\phi_0 = 2.0\ \pi$ the mean orientation $\langle\phi\rangle_T \approx 1.75\ \pi$ with the stiff contour located in the upper (left) half-space and referred to below. We analyze the migration in terms of the *mean* steady-state CSM velocity v_m^i (along the y-axis) for each half-period T_i by averaging the velocity $v_m(t)$ over T_i [47]

$$v_m^i = \langle \mathbf{e}_y \cdot \dot{\mathbf{r}}_c(\infty)\rangle_{T_i} = \frac{1}{N}\sum_{i=1}^{N}\sum_{j\neq i}\langle \mathbf{e}_y \cdot \mathbf{H}_{i,j} \cdot \mathbf{F}_j\rangle_{T_i} \ . \quad (1)$$

Eq. (1) implies that for rectilinear flows with $\mathbf{e}_y \cdot \mathbf{u} = 0$, the cross-stream transport is entirely driven by the particle drag due to the hydrodynamic backflow, induced by the potential forces $\mathbf{F}_j$. Further, the magnitude and direction of each HB (and hence of v_m^i) depend on the particle shape via the force profile $\mathbf{F}(\{\mathbf{r}_j\})$ and the dyadic mobility matrix $\mathbf{H}_{i,j}$. An expression similar to Eq. (1) can be used to determine the *mean* HI-induced flow field $\mathbf{v}(\mathbf{r})$ for each half-period [47]. The respective 2D backflow $\mathbf{v}(\mathbf{r})$, shown in Fig. 2 (a) and (b) when $\langle\phi\rangle_T \approx 1.75\ \pi$, corresponds to an *elongational* flow, which flow lines are reversed (sign change) as a result of the altering ring deformation during the $S(t)$-switching ($+\dot{\gamma} \rightarrow -\dot{\gamma}$), and displayed more clearly in Fig. 2 (c) and (d). The ring asymmetry causes generally a break of the parity symmetry (PS) of the elongational HB, but the extent of the PS-violation depends on the strength of the *mean* deformation during each half-cycle T_i [Fig. 2 (c) and (d)].

Comparing the *mean* deformation for each half-cyle, one observes that the ring asymmetry is *enhanced* during the first T_1 shear-cycle, causing an increased parity break of the elongational HB [Fig. 2 (c)]. But this implies that the *difference* between the opposing partial HB-drags at the stiff and bendy side, v_m^s and v_m^b (see [47]: Eq. (9)), becomes larger with $|v_m^s| > |v_m^b|$ since $\kappa_2 > \kappa_1$. Hence, the *mean* migration step $v_m^1 = v_m^s + v_m^b$ during the T_1-cycle is large and *positive*. In turn, during the T_2 shear-cyle the situation is reversed as the ring shape is roughly circular, i.e., the ring asymmetry is *reduced* with the result that the parity of the elongational backflow is partly recovered [Fig. 2 (b) and (d)], and the opposing partial HBs

almost cancel. The reason for the residual backflow is because the HB-drag at the stiff contour part is slightly larger than at the bendy side ($|v_m^s| \gtrsim |v_m^b|$), as a result of the larger stiffness. During the T_2-cycle the *mean* migration step $v_m^2 = v_m^s + v_m^b$ is thus small and *negative*. Over the course of one shear-cyle T, the *net* migration $v_m = v_m^1 + v_m^2$ is therefore *positive*, as displayed by all three kinds of particles [Fig. 1 (a)-(c)].

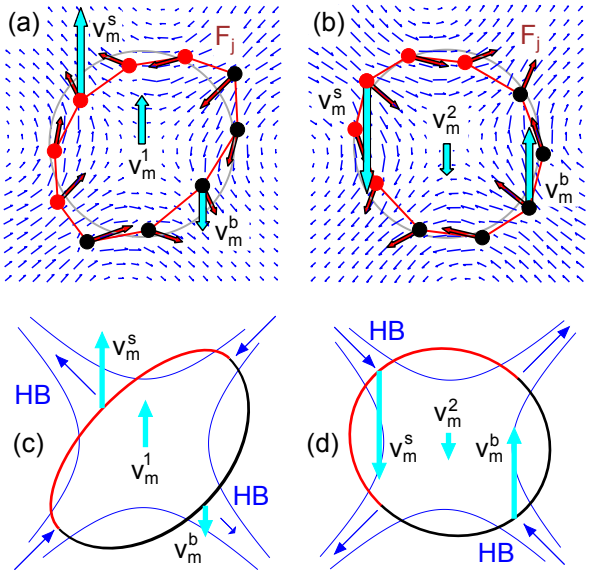

FIG. 2. (Color online) Explanation of the basic migration mechanism by way of the ring. Shown are simulation data for the *mean* ring shape, averaged over the (a) first T_1 and (b) second T_2 shear cycle, and the potential forces $\mathbf{F}_j$ along the N-bead contour. While the backflow $\mathbf{v}(\mathbf{r})$ (HB) induced within each half-cycle T_i is approximately elongational (blue), its parity is broken due to the particle asymmetry and leads to different CSM-driving drags v_m^s and v_m^b at the stiff and bendy side. Fig. (c) and (d) show how the parity asymmetry of the HB is enhanced ($|v_m^s| > |v_m^b|$) during the T_1-cycle, while during the T_2-cyle the HB-parity is partially recovered ($|v_m^s| \gtrsim |v_m^b|$), leading to a *net* positive migration $v_m = v_m^1 + v_m^2 > 0$.

Orientation Robustness. We now demonstrate that the CSM effect is quite robust against a dispersal of initial orientations by varying the angle ϕ_0, while keeping the orientation axis within the y-x shear plane. Figure 3 shows the migration velocity of the ring $\langle v_m(t)\rangle_T \tau_b/b$, averaged over one cycle T, versus time $t\dot\gamma$ ($\dot\gamma = 0.1$ fixed, $\tau_b = \eta b^3/\kappa_1$) for various orientations ϕ_0 within the intervals $I^+ = [1.1; 2.0]\,\pi$ and $I^- = [0.1; 1.0]\,\pi$. The interval I^+ (I^-) corresponds to ring orientations, where during migration the stiff/bendy part lies in the mean within the upper/lower (lower/upper) half-space. As discussed before, this implies that the final, steady-state migration velocity $v_m \equiv \langle v_m(\infty)\rangle_T$, is positive for $\phi_0 \in I^+$ and negative for $\phi_0 \in I^-$, as disclosed in Fig. 3 for $t\dot\gamma > 9.0 \cdot 10^3$. Remarkably, the ring migrates always at the same steady-state speed $v_m^{+/-}$ even though the ϕ_0-orientation varies by almost $\Delta\phi_0^{+/-} \approx \pi$, meaning $v_m^{+/-}$ is independent of ϕ_0. In turn, the choice of ϕ_0 determines strongly the short-time dynamics of $\langle v_m(t)\rangle_T$, as shown in Fig. 3 for $t\dot\gamma < 9.0 \cdot 10^3$. This imbalance of the magnitude and in part the sign of $\langle v_m(t)\rangle_T$ is a transient signature and exists as the orientation angle $\phi(t)$ is not yet in-phase with the shear signal $S(t)$; the phase synchronization of the angle takes place gradually within the transient regime over many shear cycles T before a phase-locking is established. The behavior of $\langle v_m(t)\rangle_T$, shown for the ring in Fig. 3, is generic and displayed by the other particles types [47]. We note that the migration persists ($v_m \neq 0$) when the tilt angle θ_0 between the particle axis and the y-x shear plane is non-zero [47], accentuating the robustness of the CSM effect against orientation variations. For particle orientations with $\theta_0 = \pi/2$ the upper-lower symmetry prohibits migration ($v_m = 0$) for any ϕ_0-value.

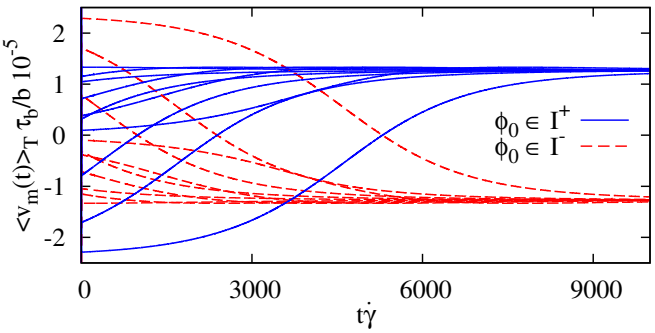

FIG. 3. (Color online) Migration velocity $\langle v_m(t)\rangle_T \tau_b/b$ of the ring, averaged over one period T, versus time $t\dot\gamma$ for different initial angles ϕ_0 taken out of the interval $I^+ = [1.1; 2.0]\,\pi$ or $I^- = [0.1; 1.0]\,\pi$. The $\langle v_m(t)\rangle_T$-transient depends on ϕ_0, while the steady-state value $v_m = \langle v_m(\infty)\rangle_T$ is ϕ_0-independent. Parameters: $\dot\gamma = 0.1$, $T = 20$, $r_\kappa = 1.5$.

Frequency Dependence. The migration process is not entirely determined by the material properties of the particle (e.g. stiffness), but can be controlled also by external parameters such as the shear rate $\dot\gamma$ or the switching period T, the latter being discussed next. Figure 4 shows the steady-state migration velocity $v_m\tau_b/b$ for a fixed $\dot\gamma = 0.1$ versus the period $T\dot\gamma$, which sets the time scale for the sign change of the shear rate $S(t)$. When $T\dot\gamma$ is small, the migration speed v_m is rather low (regime (1)) since the quickly alternating shear rate $S(t)$ induces only a small shear deformation of the ring shape, so that the ring has not sufficient time to reorient and to fully develop its mean conformation within each half-period T_1 and T_2, respectively; at these short times tank-treading is still marginal, as sketched in Fig. 4. For larger periods T, the ring has now more time within each half-cycle to deform and fully adopt the migration state, so that v_m monotonously grows first (regime (2)), approaching a maximum at $T\dot\gamma \approx 7$. At this stage, a weak partial tank-treading (TT) of the contour is initiated, but the ring dynamics is still dominated by oscillatory shear deformations, driving the CSM. Beyond a value of $T\dot\gamma > 7$ the

migration gradually decays since tank-treading becomes increasingly important insofar as a larger fraction of time of each half-cycle T_i is spent on tank-treading. This implies that a portion of the stiff/bendy contour is now partly shuffled from the upper/lower half-space to the lower/upper one (regime (3)), i.e., the dynamics of the entire shear cycle takes now place within two half-spaces (with an unequal amount) and each contributes to the CSM with opposite sign. The *net* velocity v_m is still positive, since the *mean* orientation of the ring $\langle\phi\rangle_T \approx 1.75\pi$ [Fig. 4: inset] with the stiff/bendy contour part residing on *average* within the upper/lower half-space. Beyond $T\dot{\gamma} > 11$ the CSM comes to a halt since tank-treading dominates now the dynamics within each half-period, so that even a larger fraction of the stiff/bendy contour is reshuffled between the upper-lower half-space. Within this TT-dominated regime, the *mean* orientation flips from $\langle\phi\rangle_T \approx 1.75\ \pi$ ($v_m > 0$) to $\langle\phi\rangle_T \approx 2.0\ \pi$ [Fig. 4: inset], which corresponds to a *symmetric* state where equal amounts of the stiff/bendy contour lie in the *mean* within both half-spaces, so that v_m is zero [47]. The abrupt v_m-drop is hence inherently connected with the abrupt change of the *mean* orientation $\langle\phi\rangle_T$, which can be understood by inspecting the phase-space $\langle\dot{\phi}(t)\rangle_T$-$\langle\phi(t)\rangle_T$ (see SI for details). Here we just note that the phase-space features a pattern of discrete, *asymptotically stable* orientations $\langle\phi\rangle_T^{FP}$ (fixed points), which the ring can access. Importantly, the number and value of available $\langle\phi\rangle_T^{FP}$ depend sensitively on the switching period T [47]. In our case with $\phi_0 = 2.0\ \pi$, the only stable orientation the ring can adopt is $\langle\phi\rangle_T \approx 1.75\ \pi$ as long as $T\dot{\gamma} < 11$ while $\langle\phi\rangle_T \approx 2.0\ \pi$ is unstable. This stability sequence is reversed when $T\dot{\gamma} > 11$ and the ring locks in to the now stable mean orientation $\langle\phi\rangle_T \approx 2.0\ \pi$ [Fig. 4: inset].

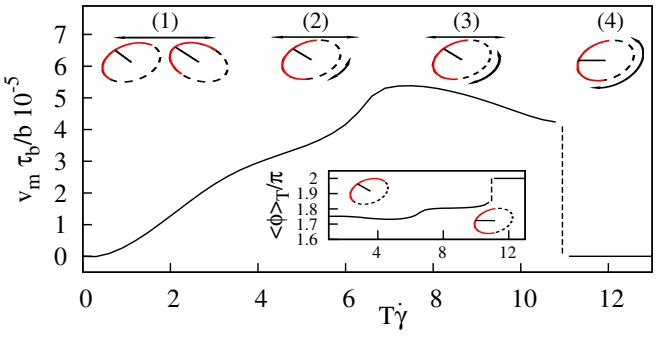

FIG. 4. (Color online) Migration velocity $v_m\tau_b/b$ of the ring versus switching period $T\dot{\gamma}$. Four dynamic regimes are identified: (1) oscillatory shear deformation, indicated by the horizontal arrow, at small T; (2) weak tank-treading (TT) superposed with (1), marked by the half-circle arrow; (3) enhanced tank-treading at large T; (4) TT-dominated with zero net migration for $T\dot{\gamma} > 11$. Inset: T-averaged mean orientation $\langle\phi\rangle_T$ vs. $T\dot{\gamma}$. Parameters: $\phi_0 = 2.0\ \pi$, $\dot{\gamma} = 0.1$, $r_\kappa = 1.5$.

Conclusions. We have shown that deformable particles, which hold an intrinsic asymmetry (parity breaking), display cross-stream migration (CSM) in time-perodic, linear shear flow. The net migration can be attributed uniquely to the particle asymmetry as it leads to an asymmetric force distribution within the periodically deformed particle, inducing asymmetric, non-compensating hydrodynamic backflows (HB). Since the magnitude and direction of the HBs depend on the actual particle deformation, which is different within the first and second half-period, the HBs averaged over one shear cycle T are nonzero, thus leading to a finite CSM [Fig. 2]. The CSM is *generic* inasmuch as it does not depend on the particle dimension nor on the specific details of its asymmetry [Fig. 1 (a)-(c)]. While the migration direction is sensitive to whether the stiff/bendy part of the particle resides during one shear cycle in the mean within the upper or lower half space, the CSM speed approaches after a transient phase a constant value and is independent of the initial particle orientation [Fig. 3].

Given that even a small asymmetry in the bending modulus (factor 1.5 or less) of micron-sized particles can trigger a sizable migration velocity of 20 μm/min under realistic flow conditions with a shear rate of $\dot{\gamma} = 22\ \mathrm{s}^{-1}$ and a period of $T = 1.75$ Hz [47], our proposed scheme facilitates appreciable migration distances in compact microfluidic setups just by independently tuning the amplitude and frequency of the shear rate. Investigating effects due to random material inhomogeneities will be an interesting subject for future studies.

Acknowledgment. PB and SG thank the Volkswagen foundation for support and gratefully acknowledge the Leibniz Supercomputing Center Munich for the provision of computing time. ML and WZ acknowledge support by the DFG priority program on Micro- and Nanofluidics.

* corresponding author: diego.kienle@uni-bayreuth.de

[1] T. M. Squires and S. R. Quake, Rev. Mod. Phys. **77**, 978 (2005).
[2] G. M. Whitesides, Nature **442**, 368 (2006).
[3] A. S. Popel and P. C. Johnson, Annu. Rev. Fluid Mech. **37**, 43 (2005).
[4] M. D. Graham, Annu. Rev. Fluid Mech. **43**, 273 (2011).
[5] J. B. Dahl, J.-M. G. Lin, S. J. Muller, and S. Kumar, Ann. Rev. Chem. Biomol. Eng. **6**, 293 (2015).
[6] E. K. Sackmann, A. L. Fulton, and D. L. Beebe, Nature **507**, 181 (2014).
[7] H. Amini, W. Lee, and D. Di Carlo, Lab Chip **14**, 2739 (2014).
[8] K. Jähnisch, V. Hessel, H. Löwe, and M. Baerns, Angew. Chem. Int. Ed. **43**, 406 (2004).
[9] K. S. Elvira, X. C. i Solvas, R. C. R. Wootton, and A. J. deMello, Nature Chemistry **5**, 905 (2013).
[10] C. Yi, C.-W. Li, S. Ji, and M. Yang, Analytica Chimica Acta **560**, 1 (2006).
[11] J. Chen, J. Li, and Y. Sun, Lab Chip **12**, 1753 (2012).
[12] R. H. Shafer, N. Laiken, and B. H. Zimm, Biophys. Chem. **2**, 180 (1974); R. H. Shafer, *ibid* **2**, 185 (1974).

[13] J. H. Aubert and M. Tirrell, J. Chem. Phys. **72**, 2694 (1980); J. H. Aubert, S. Prager, and M. Tirrell, *ibid* **73**, 4103 (1980).
[14] L. C. Nitsche, AlChE Journal **42**, 613 (1996).
[15] G. Ghigliotti, A. Rahimian, G. Biros, and C. Misbah, Phys. Rev. Lett. **106**, 028101 (2011).
[16] G. Sekhon, R. C. Armstrong, and M. S. Jhon, J. Poly. Sci. **20**, 947 (1982).
[17] P. O. Brunn, Int. J. Multiphase Flow **9**, 187 (1983).
[18] P. O. Brunn and S. Chi, Rheol. Acta **23**, 163 (1984).
[19] M. S. Jhon and K. F. Freed, J. Poly. Sci. **23**, 955 (1985).
[20] U. S. Agarwal, A. Datta, and R. A. Mashelkar, Chem. Eng. Sci. **49**, 1693 (1994).
[21] I. Cantat and C. Misbah, Phys. Rev. Lett. **83**, 880 (1999).
[22] U. Seifert, Phys. Rev. Lett. **83**, 876 (1999).
[23] H. B. Ma and M. D. Graham, Phys. Fluids **17**, 083103 (2005).
[24] S. Haber and G. Hetsroni, J. Fluid Mech. **49**, 257 (1971).
[25] L. G. Leal, Annu. Rev. Fuid Mech. **12**, 435 (1980).
[26] S. Mandal, A. Bandopadhyay, and S. Chakraborty, Phys. Rev. E **92**, 023002 (2015).
[27] B. Kaoui, G. H. Ristow, I. Cantat, C. Misbah, and W. Zimmermann, Phys. Rev. E **77**, 021903 (2008).
[28] G. Danker, P. M. Vlahovska, and C. Misbah, Phys. Rev. Lett. **102**, 148102 (2009).
[29] S. K. Doddi and P. Bagchi, Int. J. Multiphase Flow **34**, 966 (2008).
[30] V. Sibillo, G. Pasquariello, M. Simeone, V. Cristini, and S. Guido, Phys. Rev. Lett. **97**, 054502 (2006).
[31] M. Abkarian and A. Viallat, Soft Matter **4**, 653 (2008).
[32] J. Dupire, M. Abkarian, and A. Viallat, Phys. Rev. Lett. **104**, 168101 (2010).
[33] C. N. Baroud, F. Gallaire, and R. Dangla, Lab Chip **10**, 2032 (2010).
[34] J. Deschamps, V. Kantsler, E. Segre, and V. Steinberg, PNAS **106**, 11444 (2009).
[35] S. Kessler, R. Finken, and U. Seifert, Eur. Phys. J. E **29**, 399 (2009).
[36] H. Noguchi, Phys. Rev. E **81**, 061920 (2010).
[37] M. Zhao and P. Bagchi, Phys. Fluids **23**, 111901 (2011).
[38] D. Matsunaga, Y. Imai, T. Yamaguchi, and T. Ishikawa, J. Fluid Mech. **762**, 288 (2015).
[39] P. Sajeesh and A. K. Sen, Microfluid. Nanofluid. **17**, 1 (2014).
[40] T. M. Geislinger and T. Franke, Adv. Coll. Int. Sci. **208**, 161 (2014).
[41] G. Segre and A. Silberberg, Nature **189**, 209 (1961).
[42] A. Farutin and C. Misbah, Phys. Rev. Lett. **109**, 248106 (2012).
[43] N. Watari and R. G. Larson, Phys. Rev. Lett. **102**, 246001 (2009).
[44] M. Doi and S. F. Edwards, *The Theory of Polymer Dynamics* (Oxford University Press, Oxford, 1986).
[45] T. Krüger, F. Varnik, and D. Raabe, Computers and Mathematics with Applications **61**, 3485 (2011).
[46] A. Arnold, O. Lenz, S. Kesselheim, R. Weeber, F. Fahrenberger, D. Roehm, P. Kosovan, and C. Holm, *ESPResSo 3.1 - molecular dynamics software for coarse-grained models* (Springer, Berlin, 2013).
[47] The Supporting Information contains further details on the models, a derivation of Eq. (1), plots and movies on the generic behavior (including an extension of the orientation robustness) of the dumbbell and capsule, and on the SI-conversion of the capsule parameters. More background on the abrupt v_m-drop and its linkage to the $\langle\phi\rangle_T$-attractors is provided as well.